Non-Invasive Assessment of Chicken Egg Fertility during Incubation using HSSE-GC-MS VOC Profiling

Matthias Corion[a], Simão Santos[a], Nadia Everaert[b], Jeroen Lammertyn[a], Bart De Ketelaere[c], Maarten Hertog[d,1]

[a] KU Leuven, MeBioS Biosensors group, Department of Biosystems, Leuven, Belgium

[b] KU Leuven, A2H Nutrition & Animal EcoSystems (NAMES) Lab, Department of Biosystems, Leuven, Belgium

[c] KU Leuven, MeBioS Biostatistics group, Department of Biosystems, Leuven, Belgium

[d] KU Leuven, MeBioS Postharvest group, Department of Biosystems, Leuven, Belgium

[1] Corresponding author: E-mail: maarten.hertog@kuleuven.be Telephone: +32 16 32 16 14

ABSTRACT

Volatile organic compounds (VOCs) carry crucial information on chicken egg fertility. Assessing fertility before incubation holds immense potential for poultry industry efficiency. Our study used headspace sorptive extraction-gas chromatography-mass spectrometry to analyze egg VOCs before and during the initial 12 incubation days. A total of 162 VOCs were identified. Hexanal was significantly higher in unfertilized eggs, whereas compounds such as propan-2-ol, propan-2-one, and carboxylic acids were higher in fertilized eggs. Furthermore, the obtained multiple logistic regression model outperformed the PLS-DA model, demonstrating lower complexity and superior performance. Fertile eggs were accurately identified in the validation set in 68% to 75% of the cases during the initial 4 days, to 85% and 100% on days 6 and 8. Finally, hierarchical cluster analysis revealed novel insights into the emission dynamics of fertilized eggs, providing additional support for comprehending biological information encoded in VOCs and their connection to biochemical processes in developing embryos.

KEYWORDS

Fertilization status, hatching eggs, Volatile Organic Compounds (VOCs), HSSE-GC-MS, PLS-DA, Multiple logistic regression, Hierarchical cluster analysis

1. INTRODUCTION

Volatile organic compounds (VOCs) from avian hatching eggs are known to carry biological information concerning breed origin [1,2], sex [3–6], and fertility [3,7]. Particularly, acquiring details about both the sex and fertilization status would result in significant improvements in commercial incubation procedures. In specific sectors where only one sex is preferred for commercial purposes, *in ovo* sex determination would offer distinct advantages [8]. In addition, all segments of avian production stand to gain from early identification of fertilization status, ideally before incubation. This would prevent the wastage of eggs and incubation energy, free up more space in the incubator for viable hatching eggs, and therefore hold the potential for significant economic gains [9].

The literature outlines various non-destructive methods for determining the fertilization status of chicken eggs in a relatively early phase. Typically, these methods yield accurate results on approximately days (d) 4 and 5 of incubation [9]. Dielectric measurements using capacitor plates on eggs delivered a prediction accuracy of 92.3% on d 5 [10]. Electrical conductivity is relatively cheap and fast to measure and can be implemented in the incubator. In a second approach, machine vision images from backlit eggs offered prediction accuracies of 67.6%, 93.5%, and 93.9% on d 2, 3, and 4, respectively [11]. Visible transmission spectroscopy yielded a perfect prediction accuracy of 100% on d 4 [12,13]. Finally, using hyperspectral imaging, Smith *et al.* [14] achieved accuracies of 71%, 63%, 65%, and 83% on d 0, 1, 2, and 3, respectively. Furthermore, Liu and Ngadi [15] reported accuracies of 100%, 78.8%, 74.1%, 81.8%, and 84.1% on d 0, 1, 2, 3, and 4, respectively. Fertility assessment on d 0 holds the most promise as it allows for evaluation prior to incubation. However, the authors

caution that this encouraging finding requires additional validation through conventional supervised learning algorithms, as noted in a subsequent review article [9].

So far, no robust method has been established to ascertain egg fertility pre-incubation or earlier than d 3 or 4. Therefore, a deeper exploration into the viability of VOC analysis is warranted. Webster *et al.* [3] pioneered the exploration of the discriminatory capabilities of VOCs in distinguishing between unfertilized (UF) and fertilized (F) eggs. In this study, significant differences between UF and F quail-hatching eggs were observed on d 8, while no significant distinctions were found on d 1. In contrast, Xiang et al. [7] successfully managed to determine the fertilization status of chicken hatching eggs on d 0. Both studies enclosed hatching eggs individually in glass jars and extracted the headspace after a designated incubation period using solid-phase microextraction (SPME), followed by analysis using gas chromatography-mass spectrometry (GC-MS). Additionally, Xiang et al. [7] validated their measurements with an electronic nose device, which presents a more cost-effective option for industrial application.

The potential for non-destructive VOC fertilization status discrimination on d 0 has thus been demonstrated. However, as the authors conclude, further research is required to gain a deeper understanding of the biological information encoded by VOCs emitted from hatching eggs [7]. Moreover, VOC assessments on hatching eggs were conducted solely on specific days during incubation (d 0, 1, and 8) leaving a considerable gap in understanding the overall dynamic trends of VOC emissions from hatching eggs. Furthermore, the question remains whether biomarkers identified at the onset of incubation would exhibit the same discriminatory efficacy between UF and F eggs on a later incubation day. Establishing consistent biomarkers across different incubation days to determine fertilization status would significantly enhance the robustness of the discrimination model.

Hence, the objective of this study is to characterize VOCs emitted by chicken-hatching eggs over the initial 12 days of incubation. Therefore, *Isa Brown* eggs were incubated and their VOC profiles were monitored using headspace sorptive extraction-gas chromatography-mass spectrometry (HSSE-GC-MS). Fertilization prediction models were developed and VOCs from F eggs were characterized to link with embryo development. These findings offer valuable insights into the viability of predicting fertilization status using VOCs, as well as the variations in VOC emissions throughout the incubation process.

2. MATERIALS AND METHODS

2.1.Egg Samples

Isa Brown hatching eggs from 65 weeks old layers were purchased from Hatchery Verhaeghe – Het Anker (Wervik, Belgium). The eggshells were inspected for damage or dirt and were cleaned with water and paper wetted with ethanol (99.8%, Thermo Fisher Scientific, Waltham, MA). Next, the eggs were left to air-dry and numbered using a pencil. A total of 50 eggs were selected with similar egg weights (61.4 ± 1.8 g). The eggs were not older than 5 days before incubation started and they were stored at 18 °C and minimally 60% relative humidity.

The eggs were incubated under standard conditions (37.7 °C and 55% relative humidity) in an RCOM Maru 380 max (Autoelex Co. Ltd., Deokam-ri, Republic of Korea). During the process, they were tilted every hour, and VOC measurements were performed on incubation days 0, 2, 4, 6, 8, 10, and 12. On days 0, 2, and 4, a total of 42 eggs was measured. The eggs were pre-heated for 2 h before measurement on d 0 to reach 37.7 °C. Starting from d 6, an additional 3 eggs were included to augment the number of UF eggs. The fertilization status of these additional eggs was estimated by candling. On d 14, the eggs were removed from the incubator to visually assess fertility and day of death with breakout analysis, following the guidelines from the hatchery practice manual of Aviagen (Huntsville, AL; Tullet [16]). After the breakout, living embryos were decapitated with sharp scissors. The performed experiment was approved by the Animal Ethics Committee of the KU Leuven under project number ECD P025/2019.

2.2.Headspace Incubation and Extraction

Figure 1 presents an overview of the different steps executed for performing egg VOC measurements. Inert materials such as glass and stainless steel were used to minimize the background signal for the VOC measurements. For the headspace accumulation, eggs were individually enclosed in custom-made airtight glass jars with an average volume of 135 mL. Before enclosing the egg inside the jar, a stainless steel grid holder was placed on top of the egg with a Gerstel polydimethylsiloxane (PDMS) Twister® (Gerstel, Mülheim an der Ruhr, Germany). These 1 cm long sorbent stir bars had a 1 mm thick PDMS coating. Prior to the experiment, the Twisters® were conditioned following manufacturer guidelines. This grid holder configuration ensured that every Twister® was securely positioned at a fixed grid-thick distance from the eggshell. After placing an egg inside the jar, the jar was flushed with pressurized air filtered through a Donaldson® hydrocarbon filter (DF-T0050-ZK, Donaldson Company, Minneapolis, MN). Next, the airtight jars were placed in an incubator at 37.7 °C for 2 h. During these 2 h, the Twister® extracted the egg VOCs which would be subject to further analysis on the GC-MS. During the measurement session, one or two blank measurements were conducted per day as a reference for background compounds. The blank measurements followed the same protocol but without the presence of an egg. After each measurement, jars, and grids were rinsed with water and ethanol (99.8%) and dried in an oven at 100 °C.

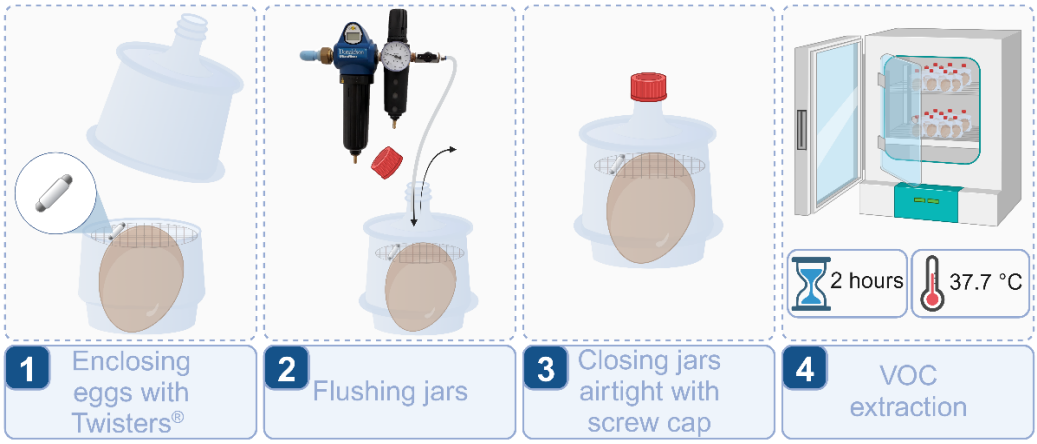

Figure 1. Overview of the different steps executed for extracting volatile organic compounds (VOCs) from eggs individually enclosed with Twister® sorbents in custom-made glass jars (figure made with BioRender.com).

2.3.Device Conditions and Data Preprocessing

The Twisters® were stored in a transport block at 21 °C for a maximum of 2 days before undergoing analysis using GC-MS. Upon being securely airtight capped, these sorbents can be safely stored for a duration exceeding one week. For the HSSE-GC-MS analysis, Twisters® were desorbed in a thermal desorption unit connected to a cooled injection system (Gerstel). Chromatography was performed using an Agilent 7890A gas chromatograph coupled to an Agilent 5975C mass selective detector (Agilent Technologies, Santa Clara, CA). The GC-MS was equipped with a 30 m × 250 µm × 0.25 µm HP-5MS column (Agilent Technologies). The device conditions for the desorption and the subsequent analysis are described in detail in [2].

The chromatograms and spectra were analyzed using MassHunter Workstation (Unknowns and Quantitative Analysis v10.1, Agilent Technologies). Initially, the chromatograms underwent deconvolution in the Unknowns Analysis and compounds were tentatively identified based on the NIST 2020 database by setting a minimum match factor of 85. The match factor assesses the resemblance between an obtained fragmentation spectrum and the theoretical fragmentation

spectra of a compound in the database. The following rules were applied to retain compounds for a custom-made library: (1) a minimum match factor of 85, (2) a higher abundance in the egg measurements compared to the blank measurements, (3) a minimum occurrence in 2 or more observations of respectively F or UF eggs on a specific day, and (4) their presence in previous in-house experiments on egg VOCs. In the second step, these compounds were double-checked for having a realistic retention index according to the order of their retention time in the chromatogram. In instances where uncertainty in compound identification arose from an unrealistic retention index or molecular mass at a given retention time, the compound was designated as “unknown" and was retained in the selection. After compound selection, a quantifier ion was chosen based on its consistent and prominent signal throughout all observations. Concurrently, an associated qualifier ion was designated to corroborate the presence of the compound. Raw quantifier ion peaks with a bell curve shape were smoothed using Gaussian smoothing, while other peaks underwent Savitzky-Golay smoothing. The signal of the corresponding compound was measured by calculating the area under the smoothed curve.

2.4.Oxygen and Carbon Dioxide Concentrations

The impact of enclosing the eggs for 2 hours on oxygen and carbon dioxide levels was assessed. Gas levels were measured on d 6, 8, 10, and 12 of incubation on 5 eggs in jars following the 2-hour incubation period at 37.7 °C utilizing a compact gas chromatograph (Interscience, B.V., The Netherlands). For oxygen analysis, the system was equipped with a PorabondQ pre-column (2 m × 0.32 mm) in tandem with a Molsieve 5A column (5 m × 0.32 mm). Meanwhile, the carbon dioxide analysis channel featured a Porabond Q column (10 m × 0.32 mm). A split flow of 10 mL/min was maintained and detection was accomplished using a thermal conductivity detector

with a helium carrier flow of 1 mL/min. Absolute concentrations were determined through the utilization of calibration curves.

2.5.Discrimination of Unfertilized versus Fertilized Eggs

In the development of fertilization prediction models, it was crucial to establish balanced calibration sets, ensuring an equal number of UF and F eggs per day. This was done to prevent the biasing of models in favor of either category. Therefore, a random subset of F observations was selected. This resulted in calibration sets of 5 observations per category on d 0, 2, and 4, and sets of 7 observations per category on d 6, 8, 10, and 12. Resultingly, the validation set consisted of the remaining F observations.

The VOC peak signals were standardized by mean subtraction and divided by the standard deviation. Subsequently, binary logistic regression models for fertilization classification were individually fitted to each VOC per day [17], followed by an evaluation of the AUC, being the area under the ROC curve (ROC: receiver operating characteristic). Following this, VOCs were selected if their models achieved an average AUC of 0.80 or higher over the 12 incubation days. From these VOCs, interaction terms were obtained by multiplying the scaled VOCs with the scaled incubation days. Similarly, these interaction terms were scaled by mean subtraction and division by standard deviation. Finally, a stepwise for-and-backward multiple logistic regression (MLR) was performed using a *p*-value threshold of 0.05 [17]. The model, built on the dataset containing all days, was assessed for its prediction performance for fertilization per day. The analysis was performed in JMP® Pro 17 (The SAS Institute, Cary, NC).

Using the same calibration and validation sets, partial least squares-discriminant analysis (PLS-DA) models were built as a second alternative to predict egg fertility [18]. Similarly, the variables

were standardized following the same procedure, and their day-interaction terms were calculated and scaled as well. Then, seven cross-validation splits were created whereby each split consisted of all the day observations of at least one UF and one F egg. The number of latent variables was determined by examining the scree plot to identify the number of latent variables. Additionally, the root mean square error plot of the cross-validation set (RMSECV) was used to identify the point where the improvement in the model became negligible. The outlier analysis was conducted by examining the Q residuals and the Hotelling T^2, and by manually checking the data for aberrant spectra. Then, the PLS-DA model was further optimized by applying a forward interval partial least squares (FiPLS), a variable selection technique whereby individual VOCs were automatically added to the model for a minimal RMSECV [19]. The multivariate statistics were performed in Matlab v2018b (Mathworks, Natick, MA) using the PLS toolbox v8.7 2019 (Eigenvector Research, Wenatchee, WA).

2.6.Patterns of VOCs over time of Fertilized Eggs

A principal components analysis (PCA) was performed on the F eggs' correlation matrix to capture the primary pattern of variability and investigate potential time dependency and correlations among variables [20]. The VOC peak signals were first normalized for the total signal of the peak areas per observation and the total signal was included as an extra variable. Next, the PCA was conducted on the F eggs dataset containing all days. The loading vectors were subsequently grouped per chemical class and the average loading vector per chemical class was calculated.

Furthermore, a two-way hierarchical Ward cluster analysis (HCA) was performed on the VOCs to investigate time pattern groupings [21]. First, each VOC was scaled between 0 and 1 across all the F eggs. Next, the VOCs were arranged in rows, with daily averages summarized in the columns. The number of clusters (CL) was ascertained from the distance graph by pinpointing the juncture at

which the rate of change in distance stabilized. Second, column clustering was performed to evaluate the dependencies between the days and the VOCs within the clusters. The analysis was performed in JMP® Pro 17 (The SAS Institute).

3. RESULTS AND DISCUSSION

3.1.Hatching Results

Out of the 50 eggs that were incubated for the experiment, a total of 42 eggs were measured up until d 4, and this total was augmented to 45 until d 12 with the endeavor to supplement the measurements with 3 additional UF eggs. However, 1 F egg was accidentally included, and only 2 UF eggs. From the assessed eggs, 3 eggs contained embryos that died on d 2, and breakout data regarding 1 egg got lost. From d 0 until d 4, 33 F- and 5 UF eggs were noted, whereas 34 F- and 7 UF eggs were recorded from d 6 until d 12. A total of 12 embryos died on d 12 probably due to the hypoxia and hypercapnia conditions induced by enclosing the eggs in a jar for 2 hours. These oxygen and carbon dioxide levels are presented in Figure 2. In preliminary experiments, it was not observed that embryos died because of measurements on d 12. Nonetheless, it is plausible that the repeated measurements of the same eggs every two days culminated in death on d 12, a point at which the stress on the embryo was at its peak due to its increased metabolic activity. For the final dataset, the eggs including dead embryos were still included since they were still alive until d 12, and no aberrant data from these eggs were observed.

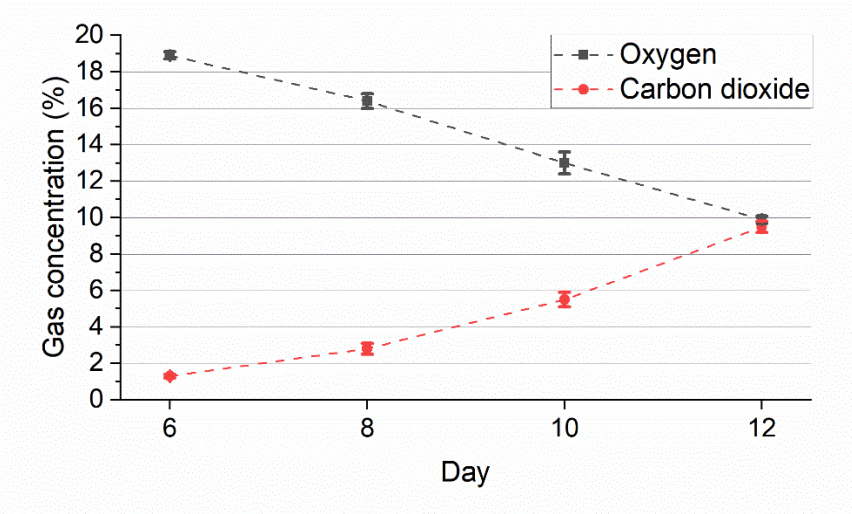

Figure 2. Averaged oxygen and carbon dioxide levels of 135 mL jars filled with an embryonated egg after 2 hours of incubation at 37.7 °C. Per day, 5 eggs were measured for their gas concentrations on incubation days 6, 8, 10, and 12. The error bars represent one standard deviation.

3.2.HSSE-GC-MS VOC Identification

A total of 162 VOCs were identified on the full dataset including UF and F eggs, which could be further categorized into 16 chemical classes (Figure 3A). The identified VOCs are reported in detail in the overview table in the Supporting Information S1. The chemical class of nitrogen-containing compounds (NCC) consisted of an imidate, an indole, an isocyanate, a piperazine, a pyridine, a quinoline, and a urea compound. Furthermore, the chemical class of sulfur-containing compounds (SCC) consisted of a sulfide, a sulfone, and a sulfur oxide. Alcohols counted the highest number of different VOCs (n = 25), followed by aldehydes (n = 23), esters (n = 22), and ketones (n = 22). In contrast to a prior study utilizing SPME fibers, the current analysis revealed a larger number of VOCs and classes. Specifically, the earlier study identified 65 VOCs from d 0 to 12 on 7 hatching eggs per day [22]. Furthermore, in other studies employing an SPME fiber for headspace extraction, notably fewer VOCs were detected. Specifically, 14 to 18 VOCs were

identified in chicken incubation eggs in research by Xiang et al. [1,5,7]. This underscores the Twister®'s capability to capture a wider variety of VOCs compared to the SPME fiber.

Next, the relative abundance of the chemical classes was studied and depicted in Figure 3B. Here, it was observed that alcohols were on average the second most abundant chemical class with an average relative abundance of 20.8% throughout the 12 incubation days. Only carboxylic acids with an average relative abundance of 27.0% were more prominent with a larger standard deviation as well. This larger variation was due to the fact that carboxylic acids increased significantly in their abundance towards d 12. This increase will be further elaborated upon in the subsequent sections.

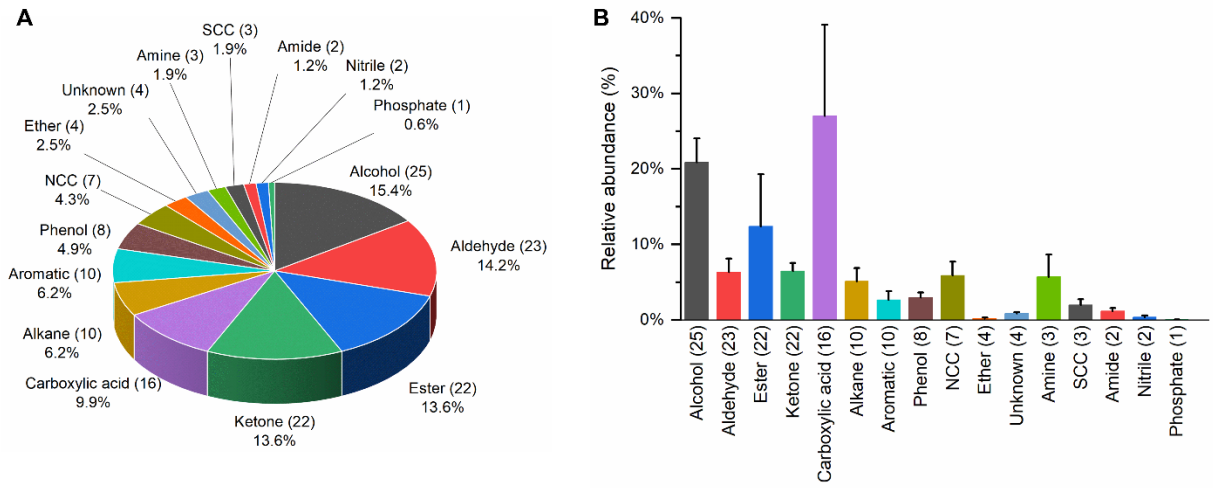

Figure 3. Distribution of the VOC data throughout 12 incubation days from the HSSE-GC-MS into chemical classes. The nitrogen-containing compounds (NCC) consist of an imidate, an indole, an isocyanate, a piperazine, a pyridine, a quinoline, and a urea compound. The sulfur-containing compounds (SCC) consist of a sulfide, a sulfone, and a sulfur oxide. (**A)** Pie chart distribution of the number of compounds per chemical class, expressed in absolute number (between parentheses) and relative percentage to the total of 162 VOCs. (**B)** The relative abundance per chemical class. The absolute number of VOCs per chemical class is presented in between parentheses, while the average relative abundance of the signal per chemical class to the total VOC signal, observed across 278 egg measurements spanning 12 incubation days, is presented on the vertical axis. The standard deviation is indicated with an error bar.

3.3. VOCs Consistently higher in Unfertilized or Fertilized Eggs

From the binary logistic regression on the individual VOCs per day, 17 out of 162 compounds were selected with an average AUC of 0.80 or higher (Figure 4). The higher the AUC on a specific day, the better the compound discriminated between UF and F eggs. It was observed that hexanal was generally higher in UF eggs and had the highest discriminative power throughout the 12 days. This result is similar to the findings of Webster *et al.* [3] and Xiang *et al.* [7] where respectively UF quail (d 1 and 8) and UF chicken eggs (d 0) had higher abundances of hexanal. Hexanal is known to be an oxidation product from n-6 polyunsaturated fatty acids such as linoleic acid [23]. During embryo development, 50% of the total yolk fatty acids are metabolized for energy, while the remaining 50% is retained in the body tissues and residual yolk of the newly hatched chicken [24]. In F eggs, it is conceivable that the partitioning towards tissue lipid synthesis led to a reduced quantity of n-6 polyunsaturated fatty acids accessible for autoxidation, resulting in a lower formation of VOCs such as hexanal.

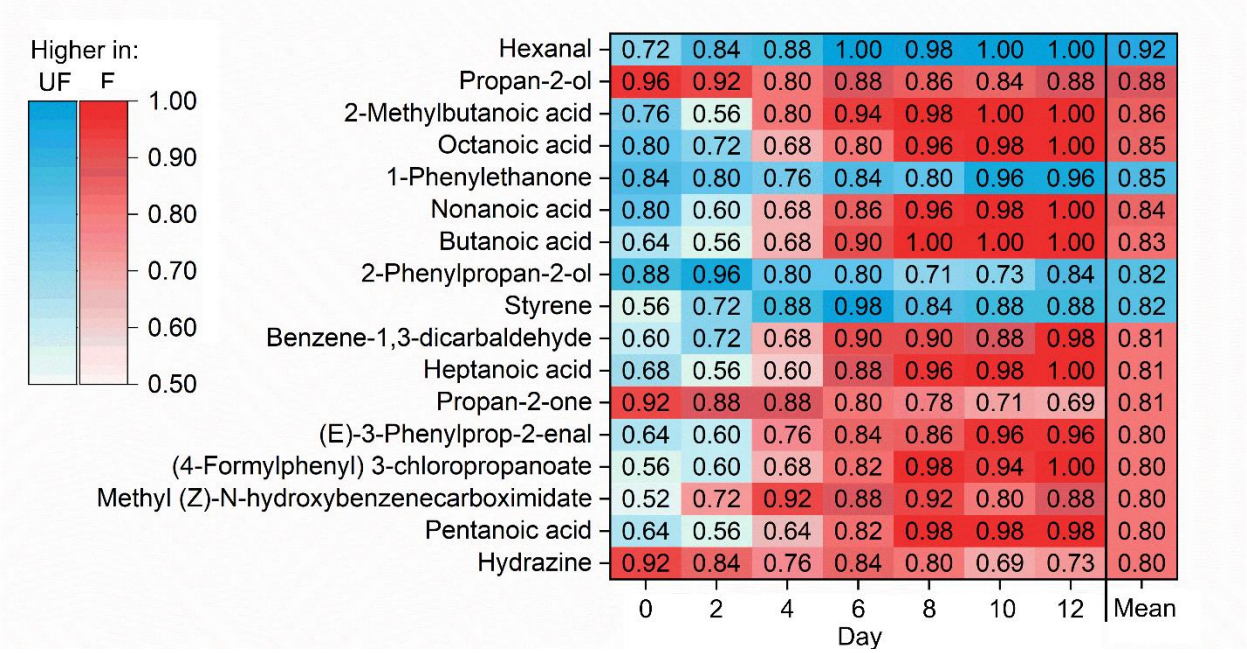

Figure 4. Heatmap of the discriminative power in the receiver operator characteristic (ROC) of the compounds with an average area under the curve (AUC) of 0.80 or higher throughout the 12 incubation days. The AUC values are depicted per incubation day with the mean value in the last column, whereas the colors blue and red correspond with compounds with a higher abundance in unfertilized (UF) and fertilized (F) eggs, respectively. For this comparison, 5 UF and F eggs were respectively used on d 0, 2, and 4. On the subsequent days, 7 UF and F eggs were used.

Moreover, propan-2-ol, propan-2-one, and hydrazine were consistently higher in abundance in F eggs throughout the 12 days with a higher discriminative power for the first incubation days. Notably, these compounds were the smallest VOCs detected in the eggs (Supporting Information S1). Considering the known capacity of microorganisms to produce hydrazine enzymatically from ammonium and nitric oxide [25], it is more plausible that propan-2-ol and propan-2-one are metabolic byproducts originating from embryonic cells. At lay, it has been approximated that the embryo may encompass as many as 60,000 cells [26]. Cell development in embryos continues after laying, although it slows down at lower temperatures [27]. As incubation initiates, there is a swift progression of cellular changes as the embryo grows [28]. Considering that cellular metabolism is active in these initial stages, it is conceivable that VOCs such as propan-2-

ol and propan-2-one could be produced as metabolic byproducts. Additionally, propan-2-ol (also known as isopropanol) and propan-2-one (or acetone) are likely associated, as propan-2-ol can be formed through an enzyme-mediated reduction of propan-2-one [29].

The early higher abundance of these three compounds in F eggs would make them interesting biomarkers to assess the fertilization status at the onset of incubation. In this study, the eggs were measured at 37.7 °C on d 0. Given the fact that these three VOCs are light in molecular mass, it is expected that they would also be detectable at room temperature. As a result, these measurements could be performed before incubation starts, allowing further usage of UF eggs for alternative purposes.

Carboxylic acids such as butanoic acid, 2-methylbutanoic acid, pentanoic acid, heptanoic acid, octanoic acid, and nonanoic acid exhibited distinctively elevated levels in F eggs toward later incubation days (Figure 4). Possibly, the hypoxia and hypercapnia conditions (Figure 2) induced oxidative stress within the egg. This oxidative stress conceivably facilitated the process of lipid peroxidation into carboxylic acids [30]. Although these stressful conditions were caused in this study by enclosing the eggs in a jar for 2 hours, it is worth noting that embryos also experience a milder degree of hypoxia and hypercapnia conditions in natural settings. This is due to the heightened metabolic activity coupled with the restricted diffusion capacity inherent to the eggshell [31]. Consequently, it is expected that F eggs will inherently generate a greater quantity of carboxylic acids as incubation progresses into later stages. However, it is suggested that dynamic headspace extractions with the provision of fresh air could alleviate the hypoxia and hypercapnia conditions. In this flow-through system, eggs would receive an influx of air, while the VOCs would be collected using a sorbent tube positioned at the outlet. Subsequently, this might yield a more accurate representation of the natural VOC emission patterns.

3.4. Construction of Fertility Prediction Models

Classification models were built to predict the fertilization status of a hatching egg during the first 12 days of incubation. Therefore, an MLR and a PLS-DA model were built and subsequently compared. The MLR served as a baseline model due to its simplicity compared to the more advanced PLS-DA model.

First, a stepwise MLR model was constructed. To enhance the model's robustness, the number of observations was enhanced by building one model across all incubation days. Additionally, the reduced set of compounds from Figure 4 was used. Through the initial reduction via this variable selection step, we aimed to address the challenges associated with logistic regression when handling a large number of variables. This is in contrast to the PLS-DA, which can manage high-dimensional and correlated data more effectively [32]. As a result, the MLR consisted of four main effects and one interaction effect (Table 1). Propan-2-ol was the highest significant parameter, followed by the interaction of pentanoic acid and day, and butanoic acid. The model unambiguously delineated that these parameters exhibited elevated values in the context of F eggs, barring pentanoic acid, for which the main effect did not attain statistical significance.

Table 1. Coefficient table of the multiple logistic regression model

Parameter	Estimate	Standard Error	Wald χ^2	*p*-value
Intercept	3.54	2.01	3.10	0.0784
Propan-2-ol	3.19	1.09	8.65	0.0033*
Butanoic acid	19.44	9.20	4.46	0.0347*
Pentanoic acid	-12.49	8.42	2.20	0.1382
Day	1.65	1.31	1.59	0.2078
Pentanoic acid × day	5.66	2.45	5.34	0.0208*

* Indicates the parameters with a *p*-value < 0.05 for the Wald χ^2 test. The Wald statistic is computed as the square of the ratio of the estimated coefficient to its estimated standard error

Similarly, a PLS-DA model was built to discriminate between UF and F eggs. Therefore, a FiPLS variable selection was applied to all the VOCs and their day-interaction effects. As a result, a model was obtained consisting of 6 factors built from 9 selected VOCs. The first 2 factors and the loadings of the selected compounds are presented in Figure 5. Similarly to the MLR model, it was noted that propan-2-ol and the interaction effect of pentanoic acid and day were also selected as significant factors in constructing the PLS-DA model. Regarding the distribution of the scores, it was noted that the F eggs exhibited a greater dispersion and displayed a day pattern, whereas the UF eggs were more evenly distributed with a less noticeable variation in the days. During early incubation, it appeared that 4-chlorophenol, methylsulfonylmethane, and propan-2-ol were selected for their higher concentrations in F eggs. In the later stages of incubation, 2-methylbutanoic acid, propanoic acid, and the interaction effect of pentanoic acid and day exhibited higher levels in F eggs. Conversely, hexanal showed greater abundance in UF eggs during the later days of incubation. This pattern aligned with the AUC values depicted in Figure 4.

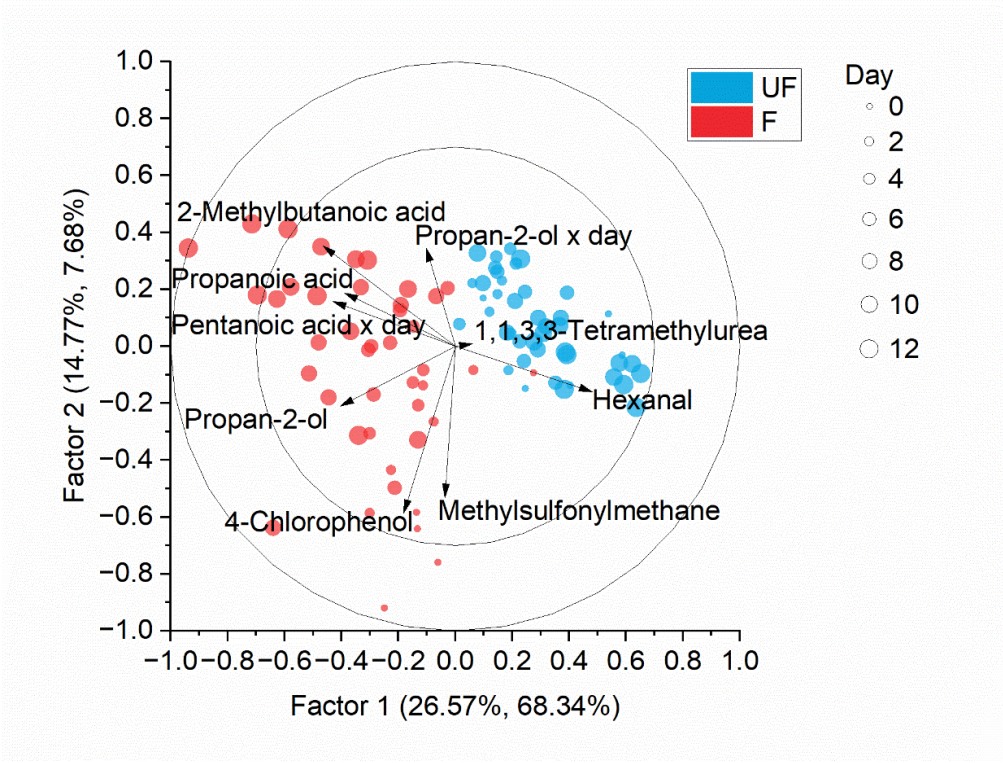

Figure 5. Biplot of the partial least squares-discriminant analysis (PLS-DA) model to separate unfertilized (UF) from fertilized (F) eggs based on their VOC profile. This model was obtained through a forward interval partial least squares (FiPLS) variable selection for which the VOCs are labeled on the biplot. The percentage of X and Y variance per factor is presented in parentheses. On d 0, 2, and 4, a combined total of 5 UF and 5 F eggs were utilized. Subsequently, on d 6, 8, 10, and 12, a combined total of 7 UF and 7 F eggs were employed to build the model. The outer and inner circles depict the 100% and 50% explained variance, respectively.

3.5. Comparison of Fertility Prediction Models

The evaluation of the MLR and the PLS-DA models involved a comparative analysis of their respective capacities to accurately predict egg fertility within the calibration and the validation sets per day (Figure 6). Having utilized all UF eggs in conjunction with an equivalent quantity of F eggs to establish the calibration set, the validation set exclusively comprised the remaining F eggs. Upon analyzing the results from the calibration sets, it was discerned that within the MLR model (Figure 6A), individual eggs were misclassified during the initial 4 days of incubation for both classes, whereas in the PLS-DA model (Figure 6B), only one F egg was misclassified on d 0. Nonetheless,

upon scrutinizing the outcomes derived from the validation set, it was noted that a diminished number of F eggs were erroneously categorized as UF eggs up to d 6 in the MLR model. Furthermore, all eggs were accurately classified on d 8, 10, and 12 (Figure 6A). Including the fact that the MLR model was built with fewer VOCs than the PLS-DA model, and was therefore less complex, it was concluded that this model was preferred over the PLS-DA model for predicting the fertilization status.

Additionally, it was inferred that the MLR model was capable of accurately identifying F eggs in 68 to 75% of the cases during the first 4 days of incubation (validation set in Figure 6A). A more true positive rate of 85% and 100% can be obtained starting from d 6 and 8, respectively. For future experiments, it would be advantageous to include UF eggs in the validation set. This would enable an assessment of how effectively they can be distinguished from the F eggs. Ultimately, it is suggested that focusing on target scans for biomarkers consistently elevated in UF and F eggs respectively, could enhance the precision of VOC abundance level estimations. More specifically, applying an extra separation step, employing a tandem GC x GC, would improve the chromatographic separation of these compounds and thereby enhance their peak signals. Consequently, this enhancement would translate into improved accuracy for VOC-based fertilization prediction models, potentially allowing for the determination of fertilization prior to incubation. Currently, it is determined that employing state-of-the-art techniques involving imaging and visible light transmission spectroscopy, particularly starting from d 4, exhibits greater robustness with accuracies ranging from 94% to 100% [11,12].

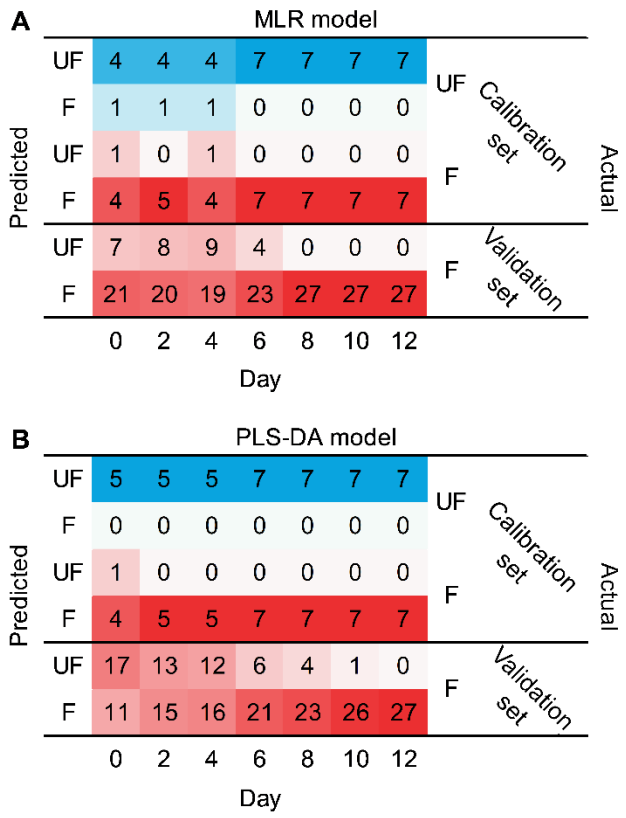

375

376 **Figure 6.** Confusion matrices of the classification models for discriminating unfertilized (UF)
377 from fertilized (F) eggs. The actual versus predicted classifications for the calibration and
378 validation sets are depicted per day. The actual UF and F eggs are colored blue and red,
379 respectively. The intensity of the color is scaled per day between 0 and the total number of
380 observations within a group. Balanced datasets were used for the calibration, whereas the
381 remaining F eggs were used in the validation set. (**A)** Multiple logistic regression (MLR) model
382 obtained through a stepwise selection with a significance threshold of $p < 0.05$. (**B)** Partial least
383 squares-discriminant analysis (PLS-DA) model obtained through a forward interval partial least
384 squares (FiPLS) variable selection method.

3.6.Patterns of VOCs over time of Fertilized eggs

As previously indicated in the biplot of Figure 5, a day pattern emerged in the distribution of the F eggs. Additionally, the significance of variables in distinguishing between UF and F eggs depended on the day. Hence, a more comprehensive analysis of these VOC patterns was conducted in F eggs through a PCA and an HCA.

A PCA was conducted on the F eggs dataset to capture the primary pattern of variability and explore potential time dependencies and correlations among variables (Figure 7). In Figure 7A, a gradual day separation was visible along the first principal component (PC) which accounted for 35.51% of the variance in the observations. Observations from earlier days (d 0, 2, and 4) exhibited more scattering compared to those from later days (d 6, 8, 10, and 12). This suggested that VOC profiles of F eggs exhibited more pronounced differences at the onset of incubation and tended to stabilize in the later stages. Next, the correlation loadings of the VOCs are presented in Figure 7B. Here, the vectors illustrate the average loading per chemical class across the first two PCs. It was noted that the carboxylic acids generally increased in abundance over time whereas the majority of the other chemical classes decreased. This latter observation was deduced from the orientation of vectors belonging to chemical classes such as ketones, alcohols, aldehydes, aromatics, esters, and alkanes pointed towards the earlier days. Finally, it was observed that there was considerable variation within a chemical class. This suggests the possibility of distinct chemical pathways within the same class. For example, alcohols and aldehydes were largely scattered along PC 2. Consequently, these distributions were subjected to a more comprehensive analysis through an HCA in the following section.

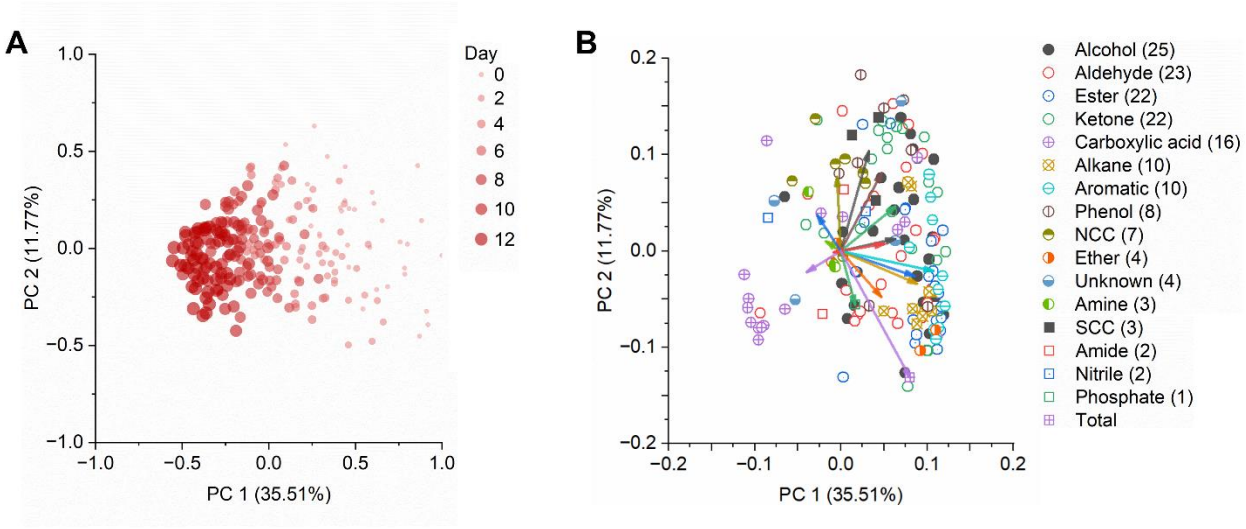

406

407 **Figure 7.** Principal components analysis (PCA) of fertilized (F) eggs throughout 12 incubation
408 days, represented along the first and second principal components (PC). (**A)** Score plot of F eggs,
409 with the size and color intensity of the symbol indicating the respective incubation day. (**B)**
410 Correlation loadings plot of the VOCs, with the geometry and color of the symbol indicating the
411 chemical class. The vectors represent the resultant loading per chemical class. The number of
412 VOCs per chemical class is indicated in parentheses.

413 A two-way HCA was conducted on the VOCs to explore temporal pattern groupings (Figure 8).
414 Utilizing the distance graph, the VOCs were categorized into 6 distinct CLs. Figure 8A presents
415 the dendrograms representing these CLs and the day CLs. In terms of day clustering, it was
416 anticipated that subsequent days would exhibit autocorrelation and consistently form clusters.
417 More specifically, d 0 and 2 were distinctively separated from the remaining days. This
418 observation aligned with what has been observed in the score plot of Figure 7A, where the early
419 days were more distinct from the later incubation days. Furthermore, the heatmap in Figure 8A
420 illustrates the average VOC abundances across time. This heatmap clearly shows that several CLs
421 encompassed VOCs with notably higher abundances, particularly on d 0 and 2 (i.e., CL 1, 2, 5,
422 and 6). The relatively higher abundance levels of VOCs in the initial days of incubation can partly
423 be attributed to the emission of external VOCs that can be absorbed by the egg post-laying and are

re-emitted at higher temperatures [3]. It is important to notice that this circumstance may pose a greater challenge in identifying biomarkers for fertilization status during early incubation that can be reliably applied to new datasets, especially in cases where eggs exhibit varying background signals.

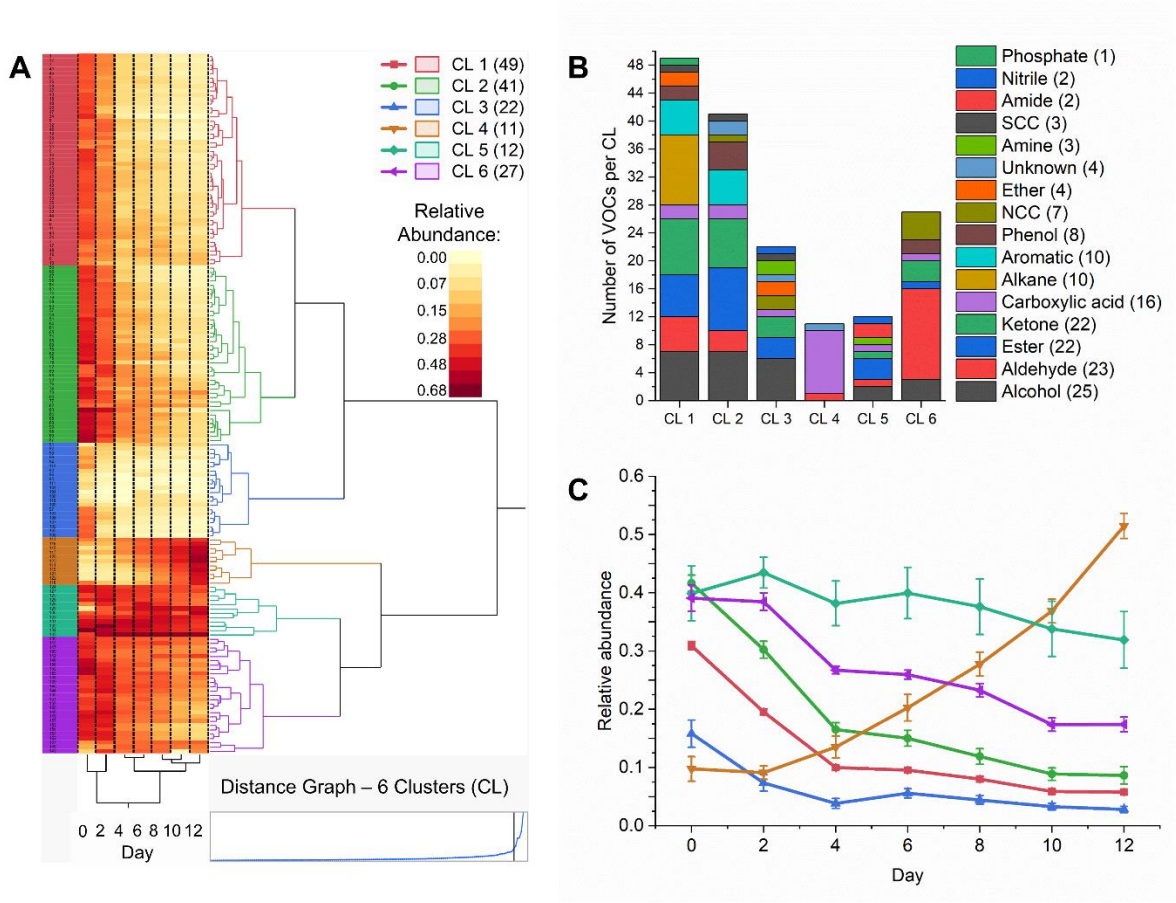

Figure 8. Two-way hierarchical Ward cluster analysis performed on the 162 volatile organic compounds of fertilized eggs. This analysis yielded 6 distinct clusters (CL), each showcasing their specific patterns throughout the initial 12 days of incubation. (**A)** Two-way dendrogram indicating the hierarchical relationships between VOCs and days, respectively. The heatmap represents the average relative abundances of the VOCs on the different incubation days. The number of VOCs per CL is indicated in between parentheses. (**B)** Column graph highlighting the distribution of the chemical classes over the different CLs. NCC stands for nitrogen-containing compound and SCC stands for sulfur-containing compound. The number of compounds per chemical class is indicated in between parentheses. (**C)** Patterns of the average relative abundance per CL over time. The error bars represent the standard error on the mean.

Next, Figure 8B displays the distribution of chemical classes across the various CLs, whereas Figure 8C visualizes the time patterns per CL. For a detailed table listing individual VOCs per cluster, refer to the Supporting Information S1. Analysis of Figure 8A and 8C revealed that CLs 1, 2, and 3 were more related to each other compared to the other CLs. These first three CLs showed relatively higher abundances in the initial two days, followed by a decline in VOC levels as the days progressed. Depending on the specific CL, a more pronounced decrease towards d 4 was observed. CLs 1 and 2 encompassed the largest quantity of VOCs, primarily comprising alcohols, aldehydes, ketones, esters, and aromatics. Specifically, CL 1 comprised all the alkanes, while CL 2 had higher numbers of esters and phenols. CL 3 had the VOCs with the lowest abundance levels and consisted mainly of alcohols, esters, and ketones. Remarkably, a slight increase in VOC abundances was observed on d 6. The overall decline in VOCs was expected to some extent, as they generally originate from amino acids, fatty acids, and carotenoids within the egg, all of which undergo degradation during egg deterioration and embryonic development [24,33,34].

Furthermore, CLs 4, 5, and 6 had more distinct patterns (Figure 8C). CL 4 consisted only of carboxylic acids, except for one aldehyde and one unknown VOC. This was the only CL that exhibited an increase over time. As previously mentioned, it was hypothesized that carboxylic acid levels increased in abundance due to oxidative stress in later incubation stages. CL 5 consisted of VOCs that were generally high in relative abundance and did not have a specific time pattern. Finally, CL 6 had a more gradual decline and maintained a comparatively higher abundance of compounds when compared to CLs 1, 2, and 3. This CL primarily comprised linear aldehydes (octanal, nonanal, dodecanal, tridecanal, tetradecanal, pentadecanal, and hexadecanal) and conjugated double-bond aldehydes ((E)-hept-2-enal, (E)-oct-2-enal, and (Z)-dec-2-enal), which can be formed through the oxidation of saturated and unsaturated fatty acids and the Strecker

degradation of amino acids [23]. In general, these findings offer valuable insights into the dynamic nature of VOC emissions in developing embryos. The clustering of compounds of the same chemical class points towards their shared biochemical origin within the egg, suggesting a promising avenue for future research.

ABBREVIATIONS

AUC	Area under the curve
CL	Cluster
F	Fertilized (eggs)
FiPLS	Forward interval partial least squares
GC-MS	Gas chromatography-mass spectrometry
HCA	Hierarchical cluster analysis
HSSE	Headspace sorptive extraction
HSSE-GC-MS	Headspace sportive extraction-gas chromatography-mass spectrometry
MLR	Multiple logistic regression
PLS-DA	Partial least squares-discriminant analysis
RMSECV	Root mean square error of the cross-validation set
SPME	Solid phase microextraction
UF	Unfertilized (eggs)
VOC	Volatile organic compound

SUPPORTING INFORMATION

Detailed overview table of the 162 identified VOCs in hatching eggs during the initial 12 days of incubation using HSSE-GC-MS.

ACKNOWLEDGMENTS

Gratitude is expressed to Elfie Dekempeneer for her support in operating the GC-MS device. This work has received funding from the Flemish Environment Department, the Foundation for Food and Agricultural Research [EggTech-0000000028], and the Research Foundation – Flanders [M.C. was funded by an SB project 1SC7219N and S.S. was funded by an SB project 1S54823N].

REFERENCES

(1) Xiang, X.; Jin, G.; Gouda, M.; Jin, Y.; Ma, M. Characterization and Classification of Volatiles from Different Breeds of Eggs by SPME-GC–MS and Chemometrics. *Food Res. Int.* **2019**, *116* (August 2018), 767–777. https://doi.org/10.1016/j.foodres.2018.09.010.

(2) Corion, M.; Portillo-Estrada, M.; Santos, S.; Lammertyn, J.; De Ketelaere, B.; Hertog, M. Non-Destructive Egg Breed Separation Using Advanced VOC Analytical Techniques HSSE-GC-MS, PTR-TOF-MS, and SIFT-MS: Assessment of Performance and Systems' Complementarity. *Food Res. Int.* **2023**, 113802. https://doi.org/10.1016/j.foodres.2023.113802.

(3) Webster, B.; Hayes, W.; Pike, T. W. Avian Egg Odour Encodes Information on Embryo Sex, Fertility and Development. *PLoS One* **2015**, *10* (1). https://doi.org/10.1371/journal.pone.0116345.

(4) Costanzo, A.; Panseri, S.; Giorgi, A.; Romano, A.; Caprioli, M.; Saino, N. The Odour of Sex: Sex-Related Differences in Volatile Compound Composition among Barn Swallow Eggs Carrying Embryos of Either Sex. *PLoS One* **2016**, *11* (11), 1–17. https://doi.org/10.1371/journal.pone.0165055.

(5) Xiang, X.; Hu, G.; Jin, Y.; Jin, G.; Ma, M. Nondestructive Characterization Gender of Chicken Eggs by Odor Using SPME/GC-MS Coupled with Chemometrics. *Poult. Sci.* **2022**, *101* (3), 101619. https://doi.org/10.1016/j.psj.2021.101619.

(6) Borras, E.; Wang, Y.; Shah, P.; Bellido, K.; Hamera, K. L.; Arlen, R. A.; McCartney, M. M.; Portillo, K.; Zhou, H.; Davis, C. E.; Turpen, T. H. Active Sampling of Volatile

Chemicals for Non-Invasive Classification of Chicken Eggs by Sex Early in Incubation. *PLoS One* **2023**, *18* (5), e0285726. https://doi.org/10.1371/journal.pone.0285726.

(7) Xiang, X.; Wang, Y.; Yu, Z.; Ma, M.; Zhu, Z.; Jin, Y. Non-destructive Characterization of Egg Odor and Fertilization Status by SPME/GC-MS Coupled with Electronic Nose. *J. Sci. Food Agric.* **2019**, *99* (7), 3264–3275. https://doi.org/10.1002/jsfa.9539.

(8) Corion, M.; Santos, S.; De Ketelaere, B.; Spasic, D.; Hertog, M.; Lammertyn, J. Trends in in Ovo Sexing Technologies: Insights and Interpretation from Papers and Patents. *J. Anim. Sci. Biotechnol.* **2023**, *14* (1), 102. https://doi.org/10.1186/s40104-023-00898-1.

(9) Adegbenjo, A. O.; Liu, L.; Ngadi, M. O. Non-Destructive Assessment of Chicken Egg Fertility. *Sensors* **2020**, *20* (19), 5546. https://doi.org/10.3390/s20195546.

(10) Ghaderi, M.; Banakar, A.; Masoudi, A. A. Using Dielectric Properties and Intelligent Methods in Separating of Hatching Eggs during Incubation. *Measurement* **2018**, *114* (November 2015), 191–194. https://doi.org/10.1016/j.measurement.2017.09.038.

(11) Das, K.; Evans, M. D. Detecting Fertility of Hatching Eggs Using Machine Vision II: Neural Network Classifiers. *Trans. ASAE* **1992**, *35* (6), 2035–2041. https://doi.org/10.13031/2013.28832.

(12) Islam, M. H.; Kondo, N.; Ogawa, Y.; Fujiura, T.; Suzuki, T.; Fujitani, S. Detection of Infertile Eggs Using Visible Transmission Spectroscopy Combined with Multivariate Analysis. *Eng. Agric. Environ. Food* **2017**, *10* (2), 115–120. https://doi.org/10.1016/j.eaef.2016.12.002.

(13) Bamelis, F. R.; Tona, K.; De Baerdemaeker, J. G.; Decuypere, E. M. Detection of Early

Embryonic Development in Chicken Eggs Using Visible Light Transmission. *Br. Poult. Sci.* **2002**, *43* (2), 204–212. https://doi.org/10.1080/00071660120121409.

(14) Smith, D. P.; Lawrence, K. C.; Heitschmidt, G. W. Fertility and Embryo Development of Broiler Hatching Eggs Evaluated with a Hyperspectral Imaging and Predictive Modeling System. *Int. J. Poult. Sci.* **2008**, *7* (10), 1001–1004.

(15) Liu, L.; Ngadi, M. O. Detecting Fertility and Early Embryo Development of Chicken Eggs Using Near-Infrared Hyperspectral Imaging. *Food Bioprocess Technol.* **2013**, *6* (9), 2503–2513. https://doi.org/10.1007/s11947-012-0933-3.

(16) Tullett, S. Investigating Hatchery Practice. Aviagen 2009. http://en.aviagen.com/assets/Tech_Center/Ross_Tech_Articles/RossTechInvestigatingHatcheryPractice.pdf.

(17) Lemeshow, S.; Hosmer, D. W. Logistic Regression. In *Encyclopedia of Biostatistics*; Wiley, 2005. https://doi.org/10.1002/0470011815.b2a10029.

(18) Barker, M.; Rayens, W. Partial Least Squares for Discrimination. *J. Chemom.* **2003**, *17* (3), 166–173. https://doi.org/10.1002/cem.785.

(19) Nørgaard, L.; Saudland, A.; Wagner, J.; Nielsen, J. P.; Munck, L.; Engelsen, S. B. Interval Partial Least-Squares Regression (i PLS): A Comparative Chemometric Study with an Example from Near-Infrared Spectroscopy. *Appl. Spectrosc.* **2000**, *54* (3), 413–419. https://doi.org/10.1366/0003702001949500.

(20) Jolliffe, I. . *Principal Component Analysis*, 2nd ed.; Springer Series in Statistics; Springer-Verlag: New York, 2002. https://doi.org/10.1007/b98835.

(21) Ward, J. H. Hierarchical Grouping to Optimize an Objective Function. *J. Am. Stat. Assoc.* **1963**, *58* (301), 236–244. https://doi.org/10.1080/01621459.1963.10500845.

(22) Corion, M.; De Ketelaere, B.; Hertog, M.; Lammertyn, J. Profiling the Emission of Volatile Organic Compounds in the First Half of Incubation. *Int. Hatch. Pract.* **2021**, *36* (1), 27.

(23) Belitz, H.-D.; Grosch, W.; Schieberle, P. *Food Chemistry*; Springer Berlin Heidelberg: Berlin, Heidelberg, 2009. https://doi.org/10.1007/978-3-540-69934-7.

(24) Lin, D. S.; Connor, W. E.; Anderson, G. J. The Incorporation of N-3 and n-6 Essential Fatty Acids into the Chick Embryo from Egg Yolks Having Vastly Different Fatty Acid Compositions. *Pediatr. Res.* **1991**, *29* (6), 601–605. https://doi.org/10.1203/00006450-199106010-00015.

(25) Kartal, B.; Maalcke, W. J.; de Almeida, N. M.; Cirpus, I.; Gloerich, J.; Geerts, W.; Op den Camp, H. J. M.; Harhangi, H. R.; Janssen-Megens, E. M.; Francoijs, K.-J.; Stunnenberg, H. G.; Keltjens, J. T.; Jetten, M. S. M.; Strous, M. Molecular Mechanism of Anaerobic Ammonium Oxidation. *Nature* **2011**, *479* (7371), 127–130. https://doi.org/10.1038/nature10453.

(26) Spratt, N. T. Role of the Substratum, Supracellular Continuity, and Differential Growth in Morphogenetic Cell Movements. *Dev. Biol.* **1963**, *7*, 51–63. https://doi.org/10.1016/0012-1606(63)90106-4.

(27) Pokhrel, N.; Sela-Donenfeld, D.; Cinnamon, Y. The Chick Blastoderm during Diapause, a Landmark for Optimization of Preincubation Storage Conditions. *Poult. Sci.* **2021**, *100* (8), 101227. https://doi.org/10.1016/j.psj.2021.101227.

(28) Kochav, S.; Ginsburg, M.; Eyal-Giladi, H. From Cleavage to Primitive Streak Formation: A Complementary Normal Table and a New Look at the First Stages of the Development of the Chick. *Dev. Biol.* **1980**, *79* (2), 296–308. https://doi.org/10.1016/0012-1606(80)90117-7.

(29) Davis, P. L.; Dal Cortivo, L. A.; Maturo, J. Endogenous Isopropanol: Forensic and Biochemical Implications. *J. Anal. Toxicol.* **1984**, *8* (5), 209–212. https://doi.org/10.1093/jat/8.5.209.

(30) Musakhanian, J.; Rodier, J.-D.; Dave, M. Oxidative Stability in Lipid Formulations: A Review of the Mechanisms, Drivers, and Inhibitors of Oxidation. *AAPS PharmSciTech* **2022**, *23* (5), 151. https://doi.org/10.1208/s12249-022-02282-0.

(31) Mortola, J. P. Gas Exchange in Avian Embryos and Hatchlings. *Comp. Biochem. Physiol. Part A Mol. Integr. Physiol.* **2009**, *153* (4), 359–377. https://doi.org/10.1016/j.cbpa.2009.02.041.

(32) Amoresano, A.; Pucci, P. Mass Spectrometry in Metabolomics. In *Metabolomics Perspectives*; Elsevier, 2022; pp 109–147. https://doi.org/10.1016/B978-0-323-85062-9.00004-0.

(33) Qiu, N.; Ma, M.; Zhao, L.; Liu, W.; Li, Y.; Mine, Y. Comparative Proteomic Analysis of Egg White Proteins under Various Storage Temperatures. *J. Agric. Food Chem.* **2012**, *60* (31), 7746–7753. https://doi.org/10.1021/jf302100m.

(34) Meng, Y.; Qiu, N.; Guyonnet, V.; Keast, R.; Zhu, C.; Mine, Y. UHPLC-Q-Orbitrap-based Untargeted Lipidomics Reveals the Variation of Yolk Lipids during Egg Storage. *J. Sci. Food Agric.* **2022**, *102* (13), 5690–5699. https://doi.org/10.1002/jsfa.11916.

595 # ABSTRACT GRAPHIC

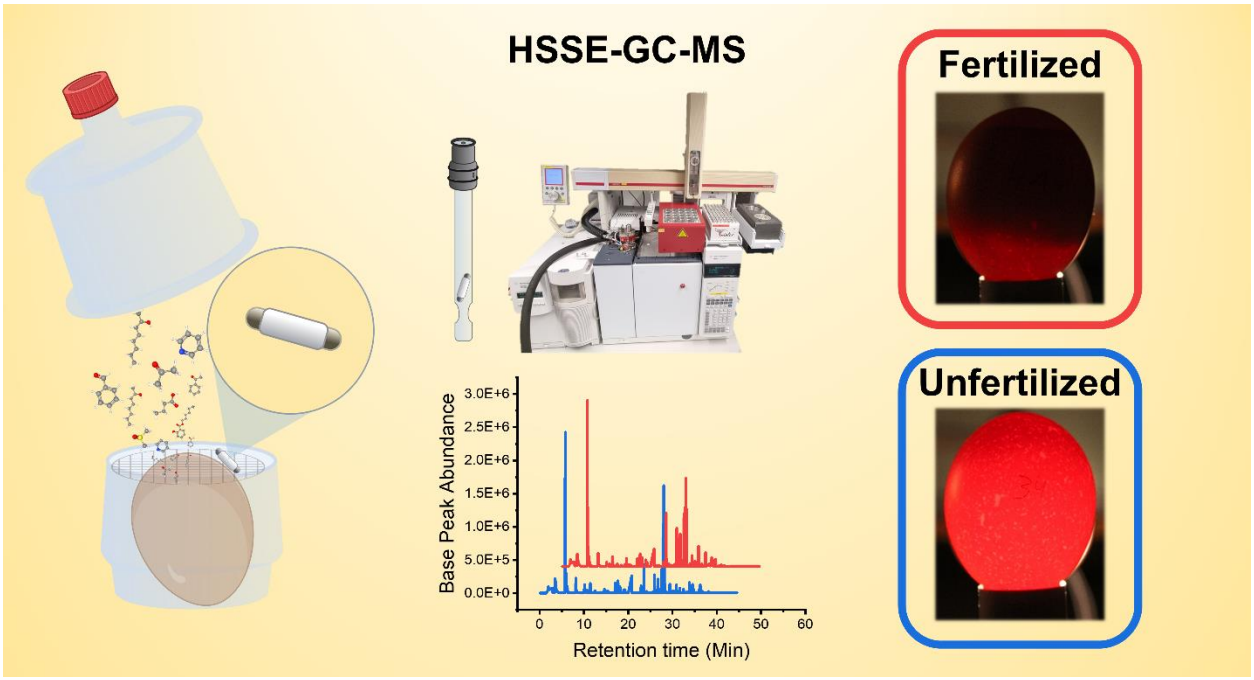

596